Design and Development of ITU pSAT II: On orbit demonstration of a high-precision ADCS for nanosatellites

Conference Paper · June 2011

CITATIONS
4

READS
1,007

13 authors, including:

Emre Koyuncu
Istanbul Technical University
80 PUBLICATIONS **423** CITATIONS
SEE PROFILE

Melahat Cihan
University of Samsun
12 PUBLICATIONS **32** CITATIONS
SEE PROFILE

Nazim Kemal Ure
Istanbul Technical University
56 PUBLICATIONS **1,049** CITATIONS
SEE PROFILE

Mehmet Caner Akay
Istanbul Technical University
6 PUBLICATIONS **24** CITATIONS
SEE PROFILE

GNC 2011
8th International ESA Conference on Guidance, Navigation & Control Systems
Karlovy Vary, Czech Republic 5 - 10 June 2011
esa European Space Agency

DESIGN AND DEVELOPMENT OF ITU pSAT II : ON ORBIT DEMONSTRATION OF A HIGH-PRECISION ADCS FOR NANOSATELLITES

Emre Koyuncu, Melahat Cihan, Kemal Ure, Caner Akay, Elgiz Baskaya, Soner Sarikaya,
Aykut Cetin, Utku Eren,Yigit Kaya, Burak Karadag, Can Kurtulus,
Prof. Dr. Metin Orhan Kaya, Prof. Dr. İbrahim Ozkol and Assoc. Prof. Dr. Gokhan Inalhan[1].

[1]Istanbul Technical University, Faculty of Aeronautics and Astronautics, Istanbul, Turkey.

ABSTRACT

ITU pSAT II is the second student satellite project from ITU FAA Controls and Avionics Laboratory, which aims to design and on-orbit demonstrate a standardized bus and a novel ADCS for pico and nano sized satellites (1-10 kg) with multi objective applications. Main aim of this project is to demonstrate specific challenges and solutions for ADCS design for nanosatellites, which require a high precision, fault tolerant and reconfigurable control system. ITU pSAT II is scheduled for launch on 2012 Q3. In this paper, we review the ITU pSAT II design including the ADCS and the software/hardware in the loop test system of ITU pSAT II. ADCS of ITU pSAT II consists of three distinct hardware layers integrating sensors, actuators, and ADCS computer over the CAN bus. The sensor layer embeds a set of low-cost inertial and magnetic sensors, sun sensors, a GPS receiver and an in-house developed multifunctional camera/star-tracker. The actuator layer includes a redundant assembly of reaction wheels, magnetic torquer coils and an experimental set of μPPTs(micro pulse-plasma thrusters). Embedded within the ADCS Computer is a filter which allows the asynchronous fusion of filtered sensor data with outputs from the orbit and attitude propagation algorithms. Propagation algorithms simulate the spacecrafts dynamical response (including effects of disturbances, and uncertainties in sensor and actuator models) and compare it with actual sensor data to improve accuracy of determination of spacecrafts attitude and orbit position. These filtered and fused state data is fed to a fault-tolerant and reconfigurable control layer. The control layer is divided into different operation modes and associated control strategies depending not only on the actual spacecraft operation mode (such as de-tumbling or high-precision attitude control for image capturing) but also depending on the health-status of the individual sensors and the actuators. This paper presents development stages of ADCS of ITU pSAT II, focusing on estimation and control algorithms and hardware implementation suited for high precision attitude control for small satellites, and development of a testbed which simulates spacecraft dynamics and space environment. Specifically, we present a software and a hardware in the loop system, which integrates components of the ADCS with an in lab developed air bearing table to simulate attitude dynamics and Helmholtz Coil system to emulate earth's magnetic field. Overall architecture is suitable for testing under number of possible hardware failure scenarios and control modes, and compensates re-design process of the system, such as improving reliability of algorithms and re-selection of hardware components.

1. INTRODUCTION

ITU pSAT II is the second student satellite project from ITU FAA Controls and Avionics Laboratory, which aims to design and on-orbit demonstrate a standardized bus and a novel ADCS for pico and nano sized satellites (1-10 kg) with multi objective applications. Main aim of this project is to demonstrate specific challenges and solutions for ADCS design for nanosatellites, which require a high precision, fault tolerant and reconfigurable control system. ITU-PSAT I, which was developed and manufactured by the same team, was launched successfully from India at 23rd of September 2009. Satellite is still known to be functional up to this date. More on the development process of ITU pSAT I can be found in [1, 5].

Nano-satellites are used and envisioned for a wide range of applications including lower-cost testing and proof-of-concept demonstration of in-development subsystems [6-9], examining of GPS signals [10], providing low-cost communication links [11, 12], taking photographs [13], and for scientific purposes such as low earth radiation measurement [14], plasma density and magnetic field measurements [12]. Beside single satellite operations it is expected in near future that groups of pico-, nano- and micro-satellites (satellite constellations) will be working as a group on orbit to perform space science [15] and service missions. Satellite constellations superiority in risk distributing risk, higher target area visit frequency, distributed measurement capability and backup ability [16] make it an ideal choice for missions such as measurement of earth's magnetic field

alterations [17] and providing lower-cost global communication services [18]. We refer the reader to [19-29] for surveys of nano-satellite applications and new nano-satellite technologies.

As indicated in [19-29], one of the bigger challenges in nanosatellite technologies is development of robust attitude determination and control systems which will allow these satellites' attitudes to be precisely known and controlled to obtain high quality mission data on demand. ITU pSAT II ADCS is envisioned to fulfill that requirement. In this paper we provide a compilation of results from [30-32] and present the design of ITU pSAT II. Specific focus is given to the ADCS hardware and software implementations suited for high precision attitude control for small satellite. In addition, we present the development of a testbed which simulates spacecraft dynamics and space environment. Specifically, the developed software and a hardware in the loop system integrates in-lab developed air bearing table and a Helmholtz Coil system to simulate attitude dynamics under on-orbit earth's magnetic field.

In Section 2, we first review the ITU pSAT II design giving insight on the bus and the subsystems. Section 3 focuses on the ADCS. Specifically the ADCS computer, sensors, actuators and the software framework is detailed. This section also includes the SIL test results from the fault tolerant and reconfigurable ADCS algorithms. In Section 4, we present an overview of the SIL and HIL that is erected for this project.

2. ITU PSAT II DESIGN

The design of ITU pSAT II hinges on a modular structure and a data bus system which allows it to be used for various types of different missions. As seen in Fig. 1, the modular structure includes a 1U (i.e. 10cmx10cmx10cm) unit PC-104 stack which embeds the system bus and a 2U (i.e. 10cmx10cmx20cm) experimental payload unit. Fig. 2 illustrates the assembly of this modular structure. The modular 3U (i.e. 10cmx10cmx30cm) structure can open up on all the side faces using hinges. This allows not only easy access to all the structural side panels, but also straight forward assembly of the payloads and components. The solar panels are screwed on the top of these side structural panels.

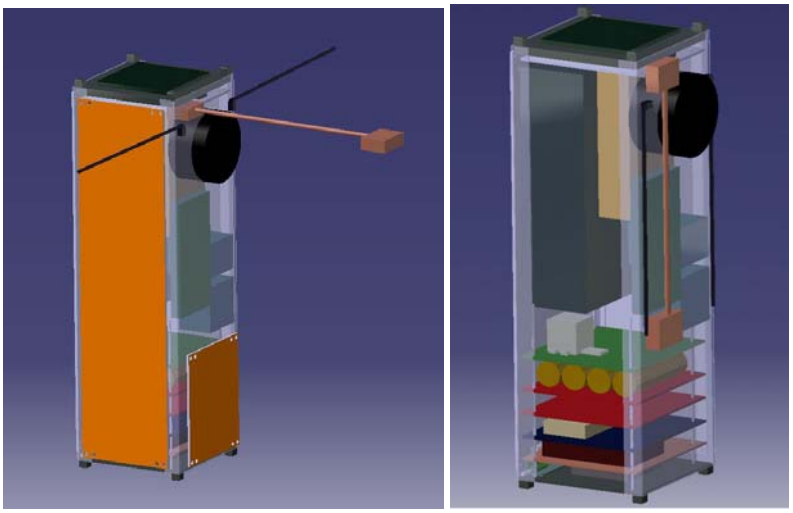

Fig. 1: *Conceptual design of the ITUpSAT II*

As designed, the ITU pSAT II structure weights less than 450 grams and it is fully compliant with Cubesat Design Specifications [32]. All the structural components are made of Aluminum 7075 T6 as it provides cheaper access and easier production in comparison to the other Aluminum grades and metals available for space usage. The modular structure is reconfigurable towards various different mission scenarios as the internal payload volume is maximized to 2U units. In addition, the payload components and boards can not only be placed horizontally but also vertically depending on size and the need for access to the side panels. The total mass and power budget is given in Table 1. It is important to note that the total power as illustrated is not the operational maximum power but only a straight power list of the all the components. In the budget, in addition to all the bus systems and specific payloads (i.e. experimental ADCS unit, the camera and the S-band transmitter) for ITU pSAT II, there is room for an additional 1000g and 5Watt (%5 duty cycle) payload room for future projects.

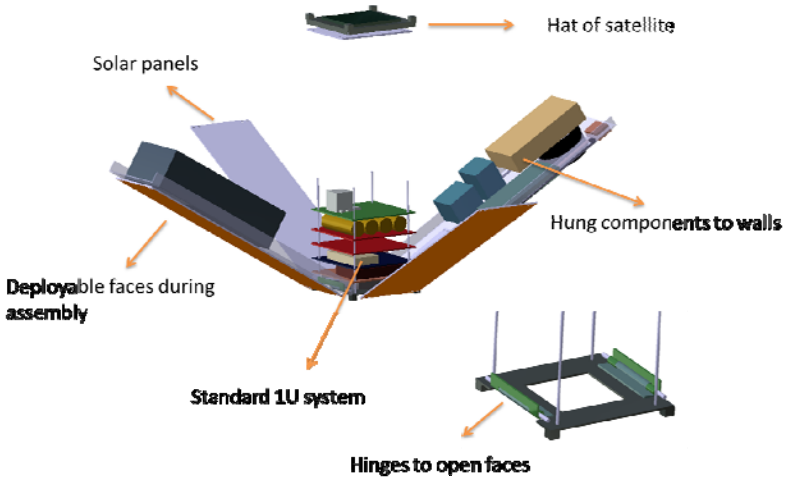

Fig. 2: *Assembly of ITU pSAT II*

COMPONENTS	Mass (gr)	Power (mW)
Structure (incl. mechanisms)	560	0
Solar Panels	660	0
Electrical Power System (EPS)	315	250
On-Board Computer (OBC)	70	250
Communication	160	10000
ADCS	550	14000
Camera	400	600
Payload	1000	5000
	3715	30100

Table 1: *Mass and power budget*

A. ITU PSAT II BUS

ITU pSAT II houses a 1U unit PC-104 stack which includes the main backbone bus of the satellite. Within the bus, an OBC, EPS, a battery board, ADCS board(including a sensor) and a GPS unit is housed. The backbone bus components are as follows:

- OBC : Aerocon NanoOBC I,
- Communication : AstroDev Li-1 UHF Transceiver,
- EPS and Battery Board : Aerocon customized Gomspace P31U-S and BP4-S units,
- GPS : SSTL SGR-05U with patch antenna,
- Solar Panels : Aerocon 3U and 1U side panels,
- Structure : AeroconNano 3U STR,
- Mechanisms : Aerocon MagBoom 3U , Aerocon AntBoom 3U, and
- Bus and cable bunde : Aerocon Kiss Bus and Cable Bundle.

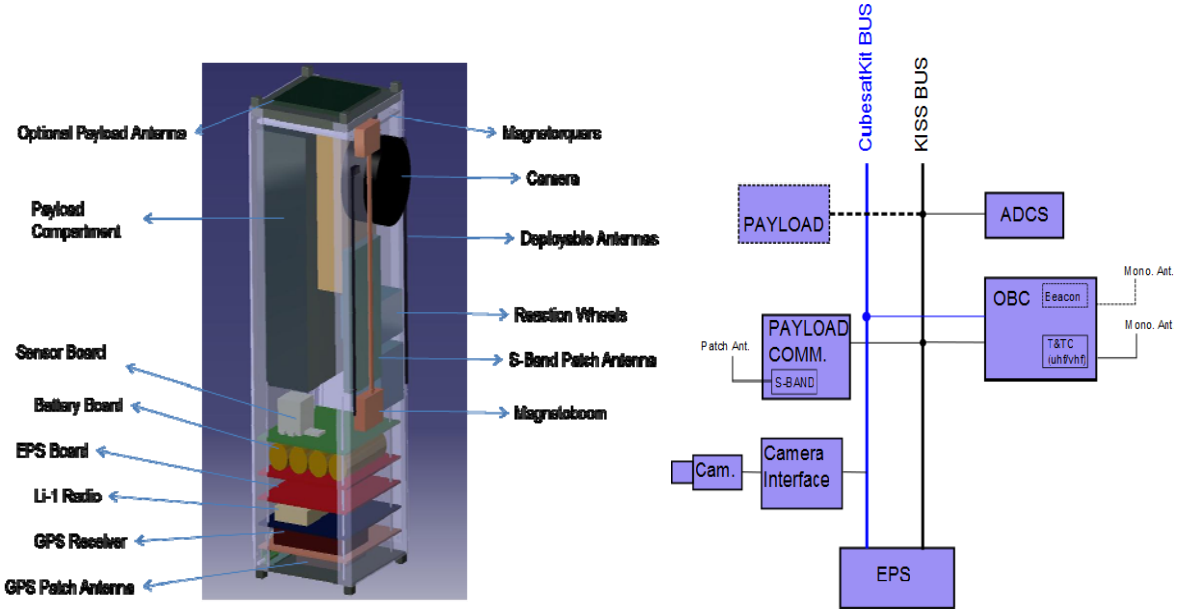

Fig. 3: *ITU pSAT II Bus – components and data bus perspective*

These units are illustrated in Fig. 3. Aerocon designation is used for the in-house and indigineous components designed under this project. The electronic system supports two different types of data buses, namely the indigenous "Kiss Bus" and the "CubeSatKit™ Bus". This is also illustrated in Fig.3. The "CubeSatKit™ Bus" has been developed by Pumpkin Inc. and has been widely accepted and used in board level OBC, EPS designs across various other cubesat OEM suppliers. In addition to the compatibility to this widely used bus, ITU pSAT II supports an indigenous "Kiss Bus" which embeds CAN bus and extra regulated power lines, providing flexibility of data rate and interface to new/payload components.

The OBC design, which is illustrated in Fig.4, implements the dual data bus and the interface to all the operation required actuators on a PIC processor. Specifically, OBC directly drives the mangetometer boom and the antenna spring loaded mechanisms. In addition embedded on the OBC unit, there is AstroDev Li-1 UHF Transceiver module. Depending on the satellite power, the transceiver module can be configured to transmit across 250mW to 4Ws at 9.6kps. This UHF uplink/downlik provides the main T&TC functionality on the ITU pSATII. In the bus stack, there is also SSTL's SGR-05U 12 Channel L1 C/A Code Space GPS Receiver which provides the satellite's position and velocity at 10m and 15 cm/s accuracy at %95 confidence interval. The EPS and the battery board of the bus are customized Gomspace P31U-S and BP4-S units respectively. As configured the EPS can provide two regulated power buses: 3.3V@5A and 5V@4A. The battery board embedds 10.4 Ah and approximately 39Wh capacity.

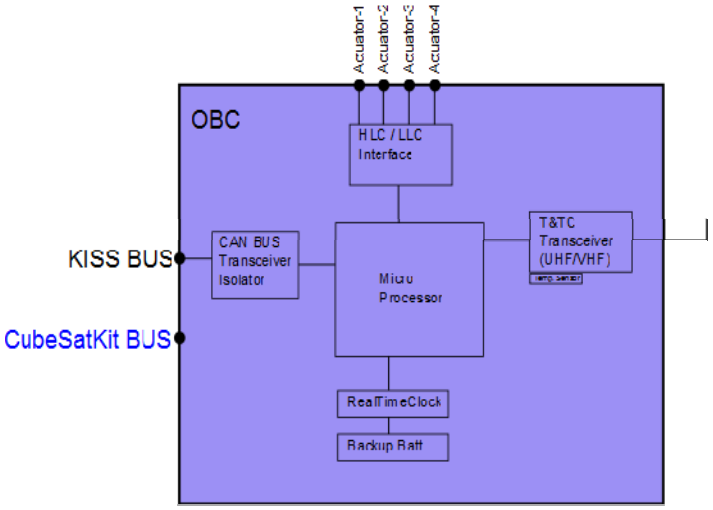

Fig. 4: *ITU pSAT II OBC design*

As illustrated the bus design of the ITU pSAT II provides a considerable amount of power, flexibility and capability with regards to carrying various types of payload units. As envisioned ITU pSAT II embeds two experimental payload units excluding the ADCS system. These units are

- Camera/Star Tracker: Aerocon customized Sony Nex-5 camera unit, and
- S-Band Transmitter: Aerocon customized AstroDev Be-1 S-band transmitter with cap antenna.

The camera system is a customized and space environment modified Sony NEX-5 unit. This compact unit embeds a 14.2 megapixel image sensor with photograph and video recording capability. The images taken by this unit are not only used for earth imaging but also star tracking and thus absolute attitude determination. The S-Band transmitter unit is a customized AstroDev Be-1 S-Band transmitter which allows us to downlink precious science and image data at speeds up to 600 kbps. This unit can be configured to transmit up to 2 Watts. In the next section, we review the hardware and the software of the experimental ADCS unit developed for the ITU pSAT II. A larger set of these results can be obtained from the group's publications [30-32].

3. ATTITUDE DETERMINATION AND CONTROL SYSTEM

A. HARDWARE LAYER

ADCS of ITU pSAT II consists of three distinct hardware layers integrating sensors, actuators, and ADCS computer over the CAN bus. The sensor layer embeds a set of low-cost inertial and magnetic sensors, sun sensors, a GPS receiver and an in-house developed multifunctional camera/star-tracker. The actuator layer includes a redundant assembly of reaction wheels, magnetic torquer coils and an experimental set of uPPTs(micro pulse-plasma thrusters).

The ADCS computer system design is illustrated in Fig. 5. The design embeds a Blackfin processor and interfaces to the dual data bus system. In addition the magnetotorquer drivers and the reaction wheel drivers are implemented on this compact unit. The ADCS computer provides analog and digital data interfaces to the sensor board and the external magnetometer which is located at the end of the boom mechanism.

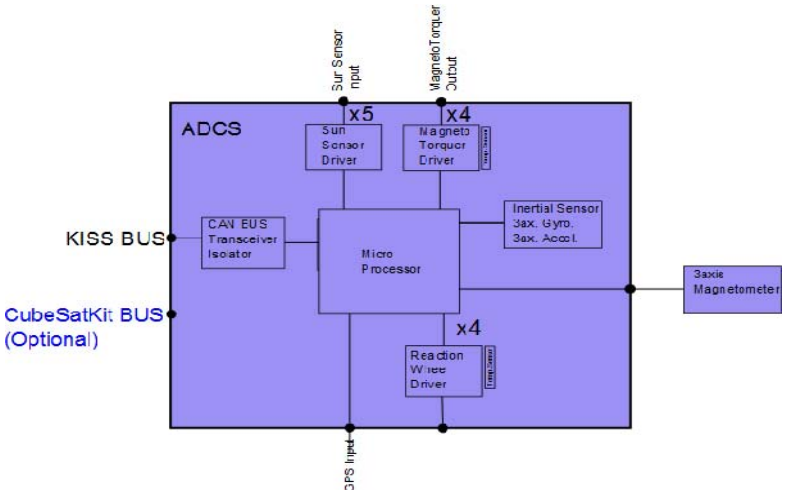

Fig. 5: *ITU pSAT II ADCS computer design*

In addition to the GPS unit which is embedded to the bus system, the ADCS houses the following attitude determination sensors :

- External Magnetic Field Sensor : Honeywell HMR 3300
- Inertial Sensor and Internal Magnetic Field Sensor : Analog Devices ADIS 16405
- Sun Sensors : Silonex SLCD-61N8 photodiodes

The complete set of sensors provide acceleration, angular velocity, internal and external magnetic field strengths on the three body axes. In addition, using the photodiodes on each panel, the panel illuminations and thus coarse sun sensing data(i.e. the sun vector) is obtained after filtering. Current actuator assembly for ADCS system consists of four magnetic torque generators and four reaction wheels completing a fully redundant set. An in-house developed μPPT system is also included only for experimental purposes including additional momentum dumping capability.

Magnetic torquers are embedded inside solar panel PCBs using layered windings. In the current design the satellite house one magnetic torquer per axis and one more additional torquer(on standard z- axis) for redundancy. The specifications of the design are given in Table 2.

Effective Area	$3.31m^2$ achieved with 13 windings in 10 layers.
Max. Dipole Moment	$0.33Am^2$ at 3.3V, 100mA

Table 2: *Magnetotorquer specifications*

The design of reaction wheels is based on requirement of being able to command the spacecraft for 1.5°/s rotation per axis. For the reaction wheels Maxon EC 20 motors are used in tetrahedron formations .The specifications of the designed reaction wheels are given in Table 3.

Angular Momentum Capability	1.05 mN.m.s
Rotor Moment of Inertia	6.23E-6 kg.m^2
Maximum Torque	1 mN.m

Table 3: *Reaction wheel specifications*

Both of the actuators provide not only redundant three axis control but also capability to overcome the estimated disturbance torques calculated for a nominal 700km sun synchronous orbit. The estimated disturbance torque values are given in Table 4.

Disturbance	**Approximate Value**
Aerodynamic Drag Induced Torque	3.6245E-08 [N.m]
Solar Pressure Drag Induced Torque	4.9212E-09 [N.m]
Residual Magnetic Field Torque	1.2800E-07 [N.m]
Factor of Safety	3
Total Disturbance with Factor of Safety	4.9295E-07 [N.m]

Table 4: *Approximate disturbance torques at 700km sun synchronous orbit*

B. SOFTWARE LAYER

The software component of the ADCS is illustrated in Fig. 6. In this architecture, the *Orbit and Attitude Propagator* simulates full dynamics of the aircraft by integrating standard spacecraft attitude equations and orbit equations with perturbations. These data along with sensor readings are sent to *Estimation and Filtering* layer, where all sensor readings and propagation data is fused to generate an accurate state vector to be fed to *Control* layer. These data are also sent back to propagation algorithms to update the current estimated state, so that they can function more precisely at the next cycle. Finally estimated states are sent to control layer, where it takes the order of current control mode from mission computer and generates commanded torque based on fault tolerant architecture. Finally commanded torque is converted into *Actuator Commands* based on actuator associated with current control mode and toque is exerted on the spacecraft. This cycle is run in every time step.

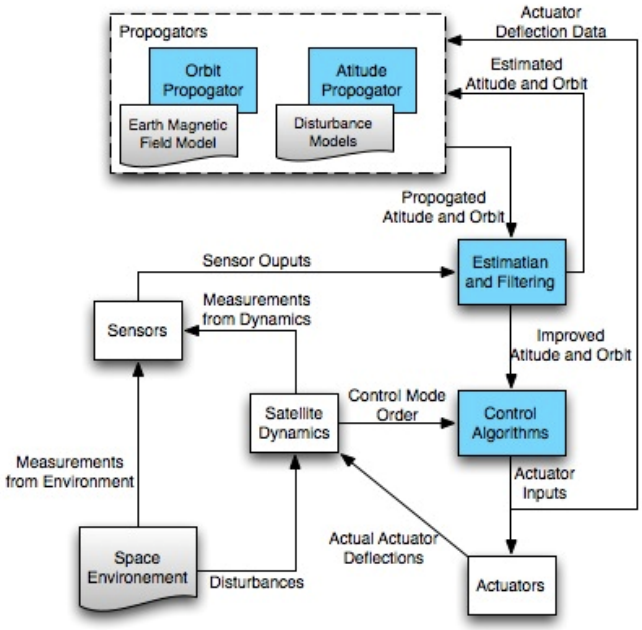

Fig. 6: *ITU-pSAT II ADCS software architecture*

Within the ADCS software architecture, we have used quaternion attitude parameterization for the model and assumed rigid body dynamics with seven variables in total (four quaternions and three dimensional angular velocity vector). In addition, the propagator also takes into account of disturbance torques on the spacecraft, which were modeled as Gaussian white noise. Order of magnitude of total disturbance also gives us a rough estimate on the necessary torque that has to be provided by actuators. Orbit propagator, simulates the orbital trajectory of the vehicle based on initial conditions provided by Tracking Location Error (TLE) file. Propagator integrates the orbital differential equations, which includes perturbation effects such as J2, in order to simulate satellites position on the orbit. This propagator algorithm also includes an *Earth Magnetic Field* model (IGRF11), which allows it to compute the magnetic field vector based on position of the spacecraft on the orbit. This satellite's position (and velocity) is estimated using the on-board GPS receiver data. Task of estimation and filtering layer is to provide noise free and reliable state data to control algorithms, which is achieved via fusion of various sensors and improvement of estimations by using a Kalman Filter. Since propagation algorithms simulates nonlinear dynamics, an Extended Kalman Filter algorithm is used in this layer, to improve efficiency of estimator on operating regions which involve nonlinear dynamics.

OPERATION MODES

Attitude control operation of the spacecraft has two modes:

1. *De-Tumbling Mode:* This mode is activated to stabilize the spacecraft's attitude from an initial high angular velocity.
2. *Attitude Tracking Mode* : This maneuvers the spacecraft's attitude from its initial position to a desired orientation.

For the "De-tumbling Mode" a nonlinear control technique namely B-Dot algorithm is used. In this mode the primary actuators are the magnetotorquers. After satellite's rotational kinetic energy is deflated, Linear Quadratic Regulator is used for to carry out the "Attitude Tracking Mode" part. In this mode the primary actuators are the reaction wheels. Embedded within the "Attitude Tracking Mode" is the momentum unloading/dumping capability which transfers the excess (and saturating) momentum on the reaction wheels using the magnetotorquers.

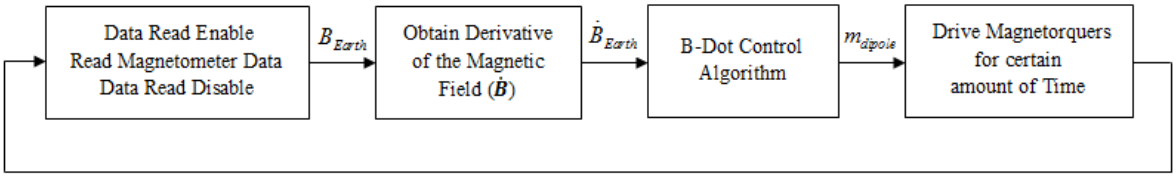

Fig. 7: *The duty cycle of the Bdot process for detumbling*

Especially after initial launch phase, spacecraft can possibly begin to spin in all directions with relatively high angular velocity, therefore have to be stabilized before entering into mission phase. Although reaction wheels can be used for this purpose, high accuracy is not needed and the wheels are likely to saturate for under high angular velocities. For this reason we prefer to use a B-dot controller, which extracts the magnetic field vector as observed from spacecraft frame from magnetometer readings, takes it derivative and feed it to magnetorquers to generate required torque, which will derive the derivative of magnetic field vector to zero. One important point on B-Dot control algorithm is obtaining the time derivative of the magnetic field. This process cannot be done with raw magnetometer data, because differentiating the magnetometer data will also differentiate sensor noises. To estimate the derivative of the magnetic field a "State Variable Filter" with cut-off frequeny is used. During stabilization, since magnetic field vectors magnitude can be assumed to be constant in the final phase, driving its derivative to zero results in driving spacecraft's angular velocity to zero. This process is illustrated in Fig. 7. Using the SIL system, which is outlined in the next section, we have tested the detumbling phase of operations across challenging scenarios. One of these scenarios is given in Table 5. Figure 8 illustrates the performance of the system under sensor noise and actuator limitations. As it can be seen from Fig. 8, the system provides stabilization just under five orbits.

Control Gain [C]	-4e4
Cut-off Frequency [ω_c]	Variable : 0.6Hz and 2 Hz
$\omega_{sat} = [\omega_x \quad \omega_y \quad \omega_z]$	[0.54 0.42 0.48] rad/s

Table 5: *Simulation parameters for detumbling scenario*

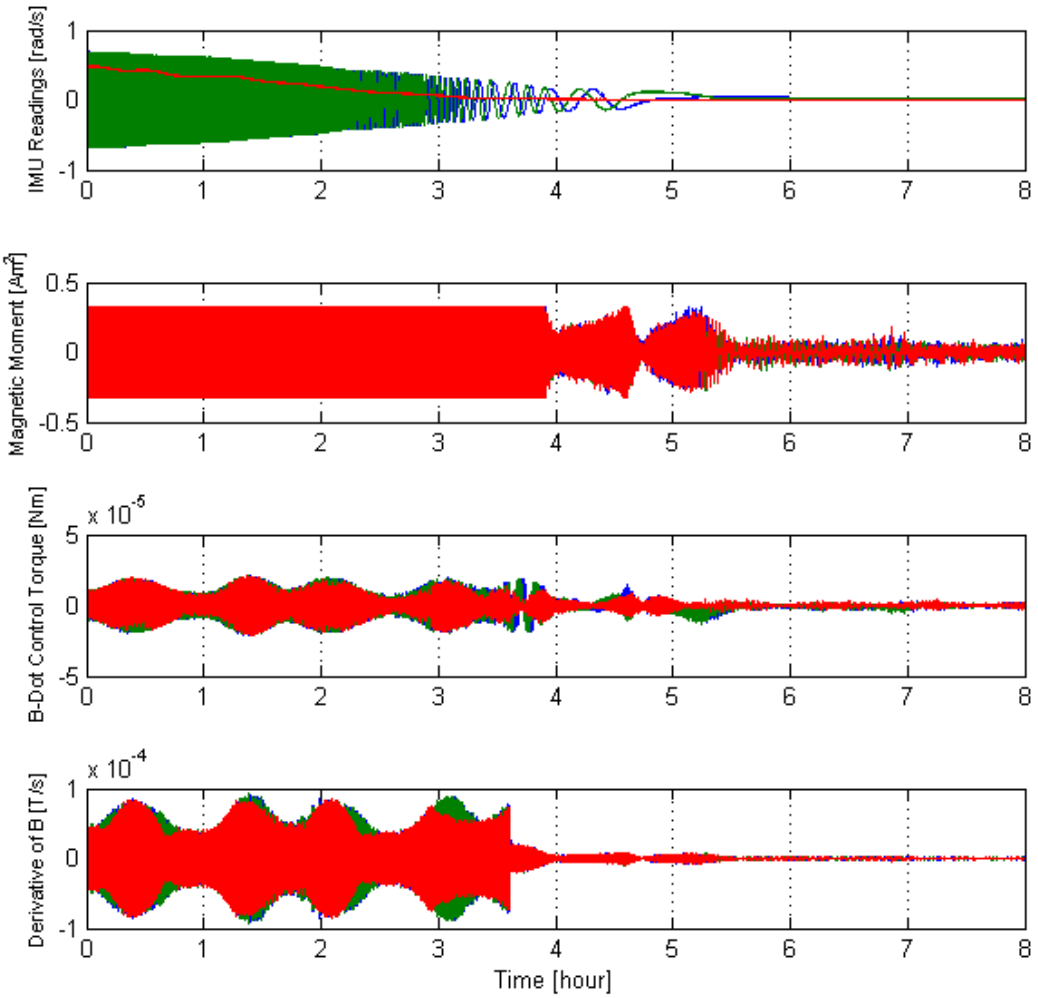

Figure 8: *Simulation Results of the scenario in Table 5.*

During simulations, it has been observed that the relatively low cut-off frequencies provide better performance at relatively low angular speeds region. In comparison, higher cut-off frequencies provide better performance at relatively high angular velocities. For that reason a variable cut-off frequency state filter is used for magnetic field rate calculations. In this scenario, reduction in cut-off frequency has been performed about three and a half hours after deployment. From that moment on, the controller has switched from 2.0 Hz to 0.6 Hz cut-off frequency. This change in cut-off frequency can be observed in derivative of magnetic field. Consequently, using two different cut-off frequencies at different phases of the detumbling operation provide high performance during the whole detumbling process.

When the spacecraft is stabilized around any attitude (via De-Tumbling Mode) then Attitude Tracking mode is used for high accuracy attitude command. Basically this mode makes use of linearized spacecraft equations and applies an optimal control method by minimizing a linear quadratic performance index (LQR). Since estimation layer includes a Kalman Filter, overall control scheme can be considered as a LQG controller. These types of control algorithms have guaranteed robustness margins and moreover, actuator saturation constraints can be embedded into performance index to avoid them. This control algorithm uses full state feedback, and makes use of redundant assembly of reaction wheels to generate desired torque. When used in vicinity of trim point controller performs well, but actuator saturation becomes harder to handle when large maneuvers are requested. To avoid the saturation on actuators, large attitude command is decomposed into a sequence of smaller magnitude attitude commands, and then the spacecraft is derived to final reference by taking each attitude

waypoint at a time. Spacecraft is commanded to translate to desired attitude from its initial position. Instead of trying to go directly commanded attitude, spacecraft is forced to follow intermediate points between initial and desired attitude. These waypoints get updated whenever spacecraft gets near to them, thus overall tracking motion is not time based but event based. Using the SIL system, which is outlined in the next section, we have tested the attitude tracking phase of operations across challenging scenarios. One of these scenarios is given in Table 6. Figure 9 illustrates the performance of the system under sensor noise and actuator limitations. As it can be seen from Fig. 9, the system provides stabilization just on the order of 100 seconds. First the system is stabilized to the nominal zero all case and then commanded to track the desired Euler angles. It is important to note the periodic momentum dumping from the reaction wheels during the whole attitude tracking maneuver which allows the system to operate safely using both of the actuators.

Initial Euler Angles	[-15 -34 43] deg
$\omega_{sat} = [\omega_x \quad \omega_y \quad \omega_z]$	[0.021 0.024 0.018] rad/s
Desired Euler Angles	[-33 57 -45] deg

Table 6: *Simulation parameters for attitude tracking mode*

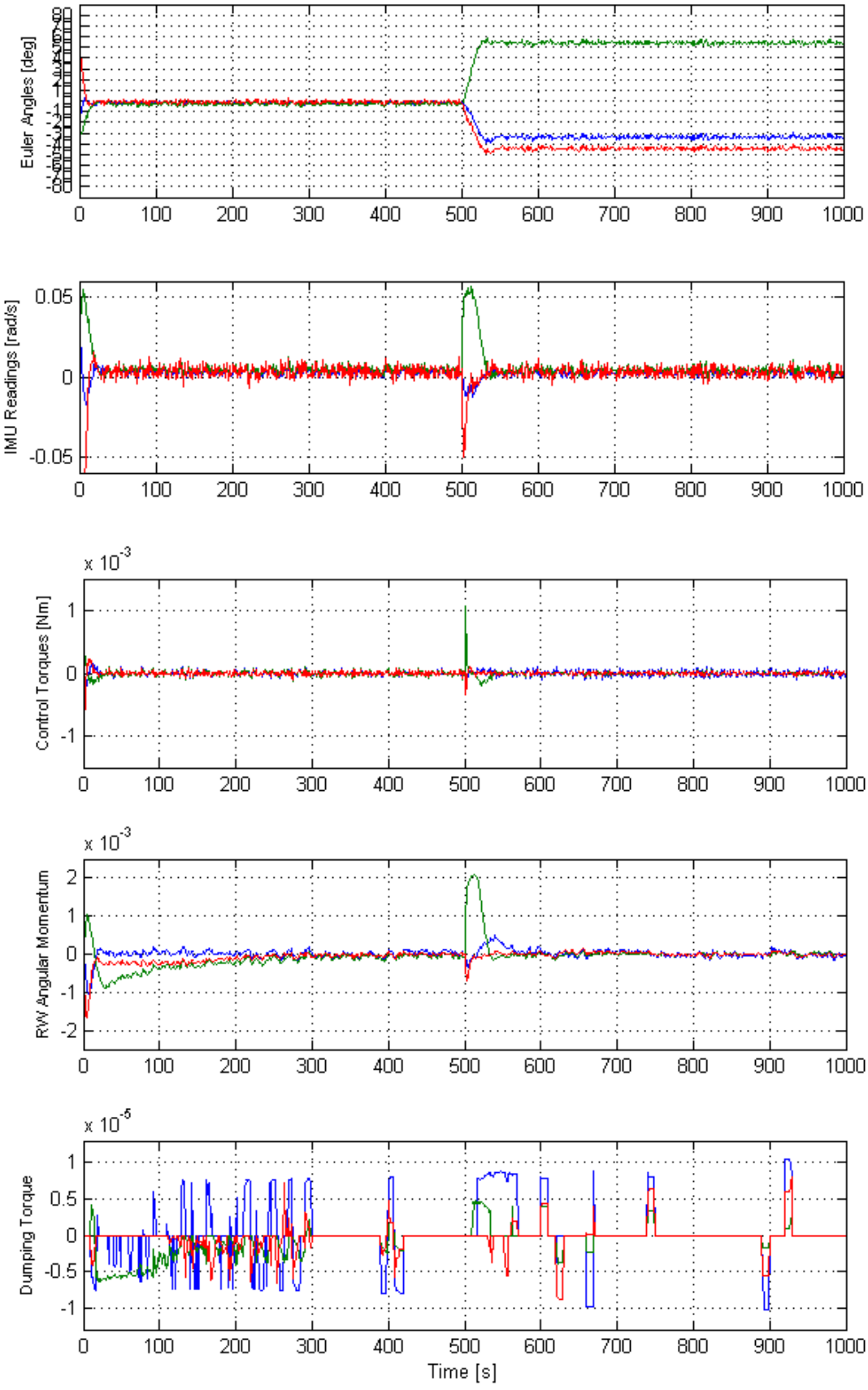

Fig. 9: *Simulation results for attitude tracking mode*

FAILURE DETECTION AND RECONFIGURATION

Given the failure-prone nature of space-tolerance increased COTS and in-house developed hardware elements, it is essential essential to a) develop on-orbit software which can detect, overcome or provide graceful degradation of performance across various failures, b) test the ADCS software hardware on ground for a complex set of hardware and software failure scenarios. ITU-pSAT II bus and ADCS operation architecture embeds a health monitoring system [30-32] in order to cooperatively detect and successfully handle the highly possible failure modes (such as sensor, actuator failures and errors). Basically the health monitoring system inspects sensed and estimated state vector to analyze if there is an error in the sensors (noise and biases in sensors have already been handled in filtering layer) or if there is a failed actuator. After detection, this system reconfigures the estimation and the control layer through mode switching to account for the errors and the failures. Reconfiguration of control architecture in case of actuator failure, performance degradation, and sensor bias has been extensively studied in terms of adaptive and intelligent spacecraft control. Design of control laws, which take into account actuator saturation and parametric uncertainty and a more extreme case of controlling spacecraft in under-actuated situations has also been of interest. On these two lines of research, we refer the readers to [30-32] for a short survey of related results.

Primary fault scenarios that we deal are actuator and sensor failures due to degradation of performance or complete shutdown at worst situation. Failure detection algorithms for sensor and actuator works independent of each other therefore it is possible to deal with a multiple failure scenario where sensor and actuator failure happens at the same time.

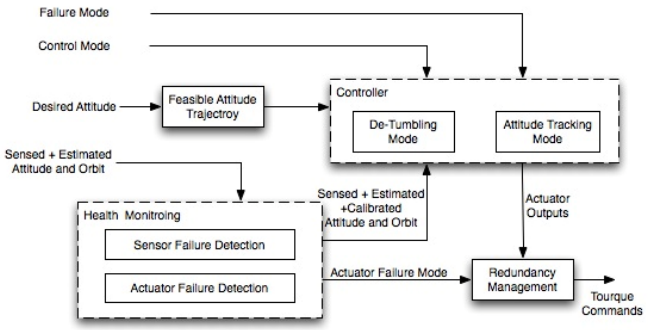

***Fig. 10** : Fault tolerant control and health monitoring system*

1. *Sensor Failure Detection :* Sensor readings, which are degraded by noise, are handled by sensing layer and estimation layer, as well as biased readings. These kinds of biases are likely to happen in accelerometers and gyros, which must be handled online in order to avoid sending false state data to the control algorithms. Filtering and estimation layer achieves bias estimation, by comparing sensed state data and state data estimated by estimation layer. It generates an initial bias estimation then updates this estimate based on difference between state vectors generated by sensor data and estimation layer. Another possible scenario is failure of sensors (either turning off or giving highly erroneous data) during mission, rendering some of the sensor useless. Sensor failure detection layer in Fig. 10 identifies the failed sensor, and isolates it from the estimation layer such that output of the failed sensor doesn't affect the performance of the estimation layer.

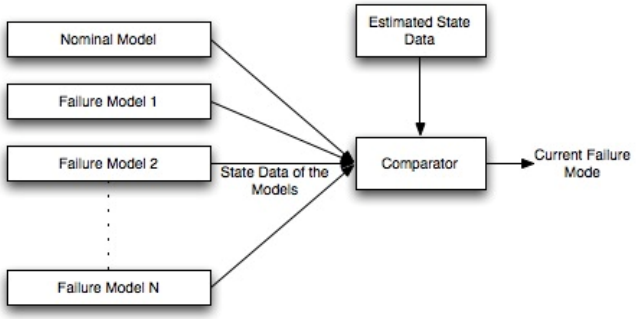

***Fig. 11** : Multiple Failure Model and failure identification*

2. *Actuator Failure Detection :* Actuator failure is possible to detect using Multiple Model Switching Scheme. This failure detection process is shown in Fig. 11. Principle of this detection algorithm is to generate state data based on all possible actuator failure scenarios (very similar to attitude propagation), and compare it with the current state data, to generate a performance index (which is integrated over time). When performance index associated with that mode is small compared to others, actual model is more likely to be in that failure mode. When minimum is taken over all possible failure data, the argument, which minimizes the performance index, indicated the failure mode of the actual system. If nominal model appears to minimize it, system continues to perform in full configuration. Whenever a failure mode minimizes the index, failure is detected and redundancy management is informed. Since an under-actuated spacecraft is very difficult to control precisely, redundant numbers of actuators are usually found in spacecrafts to take caution against actuator failures. Since all control algorithms in Fig. 11, generate a 3 dimensional commanded torque Redundancy management (sometimes referred as control allocation layer) have to distribute them among redundant actuators.

Using the failure detection, we have tested the algorithm across actuator failure scenarios at both the detumbling and the attitude tracking modes. In the detumbling mode, we assume the failure of y-axis magnetotorquer using using the identical nominal scenario as given in Table 5. In Fig. 12, the simulation results show that, even if one of magnetorquer is disabled, the satellite's angular velocity converges to zero eventhough the settling takes more time.

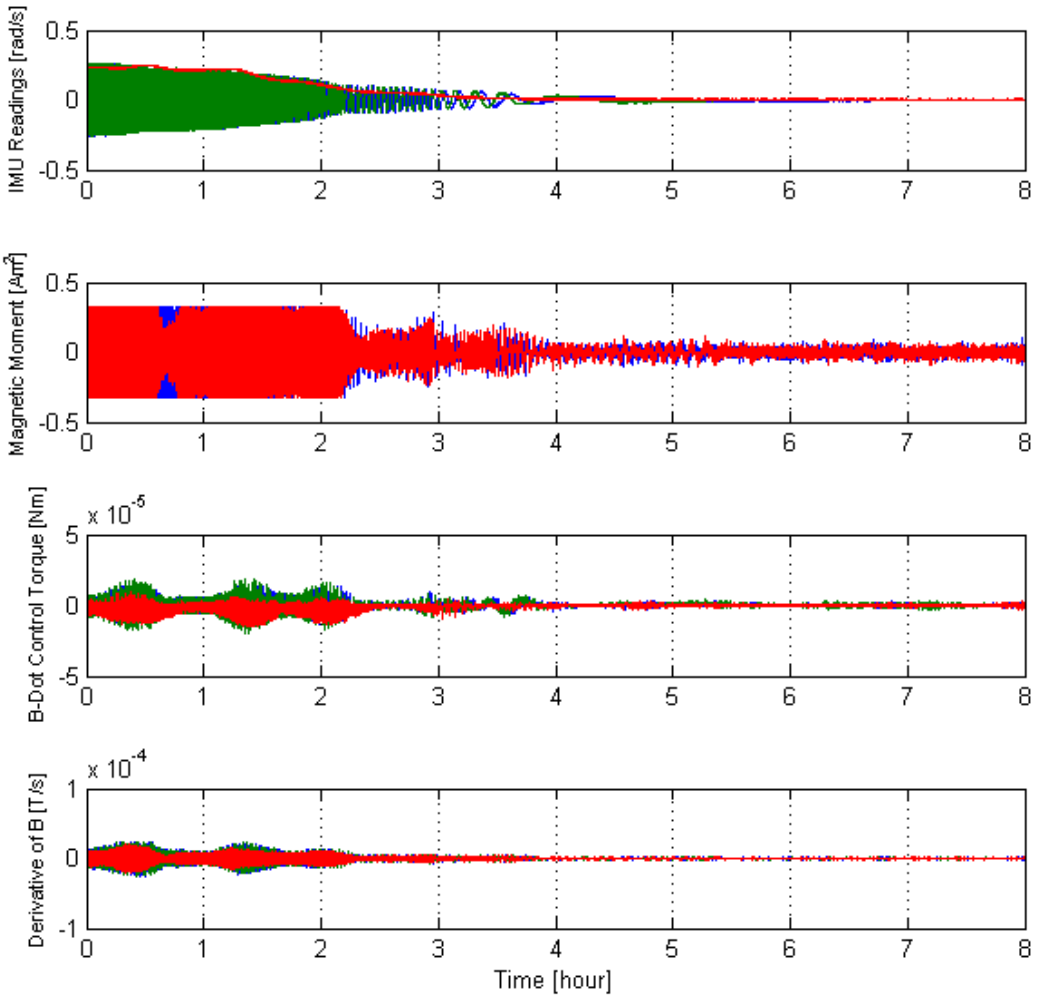

Fig. 12: *Simulation Results for y-axis magnetotorquer failure while performing detumbling*

For the attitude tracking mode, we assume that one of the reaction wheels fail during the attitude tracking maneuver scenario as given in Table 6. In Fig. 13 the simulation results show a robust performance given the the tetrahedron reaction wheel structure which provides inherent redundancy. In the next section, following [30-32], we review the HIL and SIL system developed for this project. For extended results on the SIL/HIL, we refer the readers to [30-32].

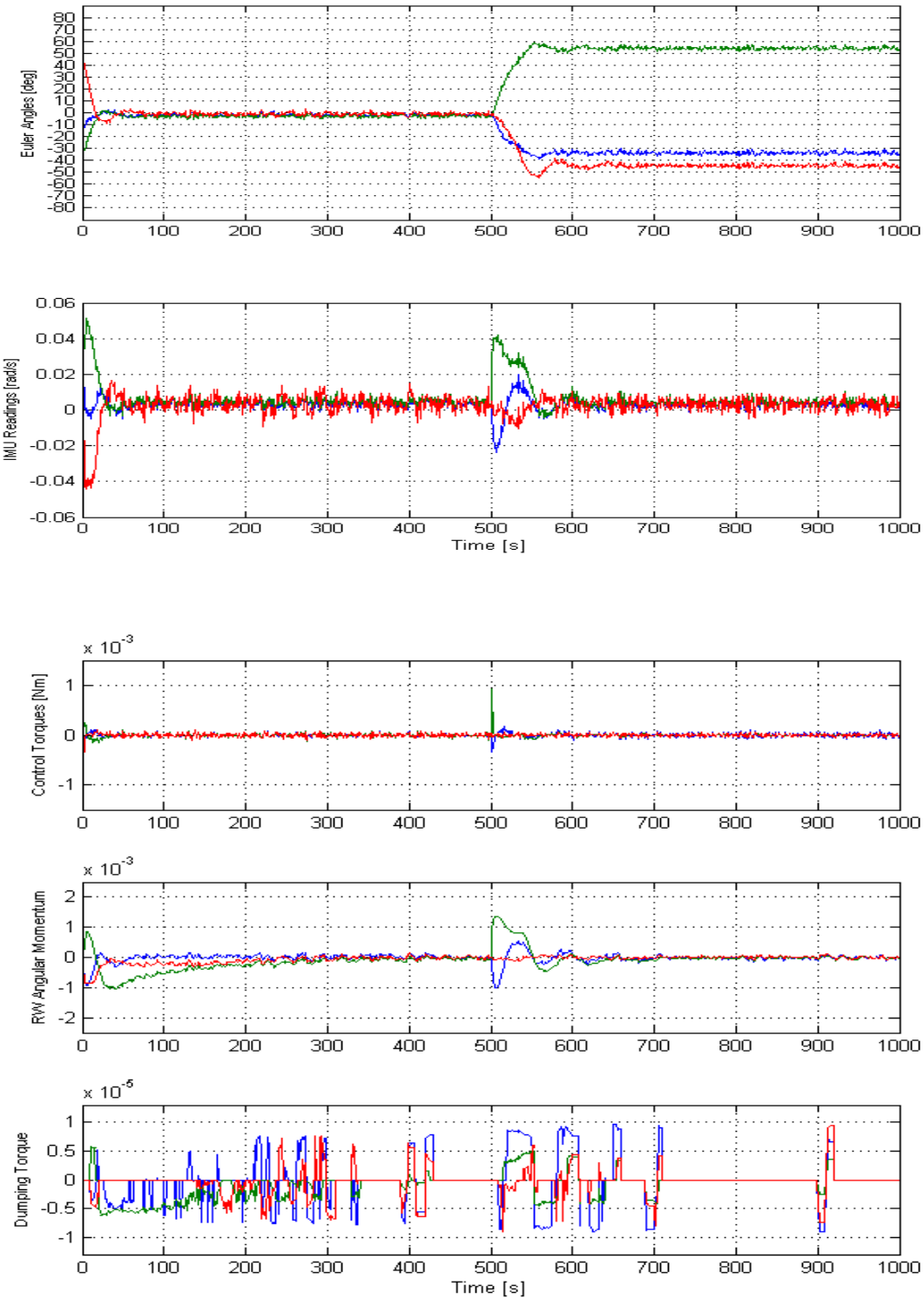

Fig. 13: *Simulation Results for one reaction wheel failure while performing attitude tracking*

3. SOFTWARE AND HARDWARE IN THE LOOP SYSTEM

To test the actual behavior of the control system elements during execution of real mission of the spacecraft including failure scenarios, we have developed a software and hardware-in-the-loop test system. The software and hardware-in-the-loop system consists of an in-house developed air bearing table (to simulate attitude dynamics) and Helmholtz Coil system (to emulate Earth's magnetic field) in addition to the computer rack which provides high-precision orbit, attitude and environment "truth-model" propagation with 3D orbit and attitude visualization. Overall architecture is suitable for testing under number of possible hardware failure scenarios and control modes, and greatly aids the development process of the ADCS and bus components. Particular difficulty with this situation is how to make a develop a "truth model" which will act as the actual state of the spacecraft in the space, and will be tried to estimate as good as possible by filtering layer and sensor emulations. It is pointless to use models in attitude and orbit propagators as truth models, since this situation will not present any interesting results due to indifference between estimated and actual states other than disturbance. For this purpose we incorporate a commercial space mission simulator "Satellite Toolkit" (STK) developed by Analytical Graphics Inc. into our simulation setup. Satellite Tool Kit is widely used software for developing and analyzing virtual space missions. STK can be used for calculating contact time between ground and satellite, determining critical vectors such as magnetic field vector and determining other attitude information rapidly by communicating with a MATLAB/Simulink model. STK serves as a truth model since it takes into account disturbances and perturbations from large number of sources and uses mathematical models far more complex than the ones we used in propagation algorithms. In addition since it is possible to extract the actual state data from STK we can see how well estimation layer works.

A. SOFTWARE-IN-THE-LOOP SYSTEM ARCHITECTURE

Components of SIL simulator are shown on Fig. 14. A cycle of simulation can be explained as follows: ADCS software (including propagation, filtering and control algorithms) is provided either by an interface in STK Rack (INT) or by some outside source, such that anyone with an ACDS software can connect to simulation setup and test his/her algorithms. Software receives state update from STK over UDP channel, sensor emulation (such as noisy readings, magnetometer calibration errors, gyro biases) are applied to state vector to simulate actual sensor reading during mission. Based on these data ADCS software applies the filtering and control architecture detailed in second section to generate commanded torques to spacecraft and sent (via CAN Bus in INT, via UDP in outside source) to STK software to simulate its effect on spacecraft model. Communication between ADCS software (which is modeled in MATLAB Simulink) and STK is achieved through another Simulink model in STK computer, which also adjusts the synchronicity between the software. Finally STK open a special 3D visualization window to observe attitude and orbit of the test spacecraft and this visualization is displayed via a projector. In in Fig. 14, a STK screenshot from an SIL simulation is also displayed.

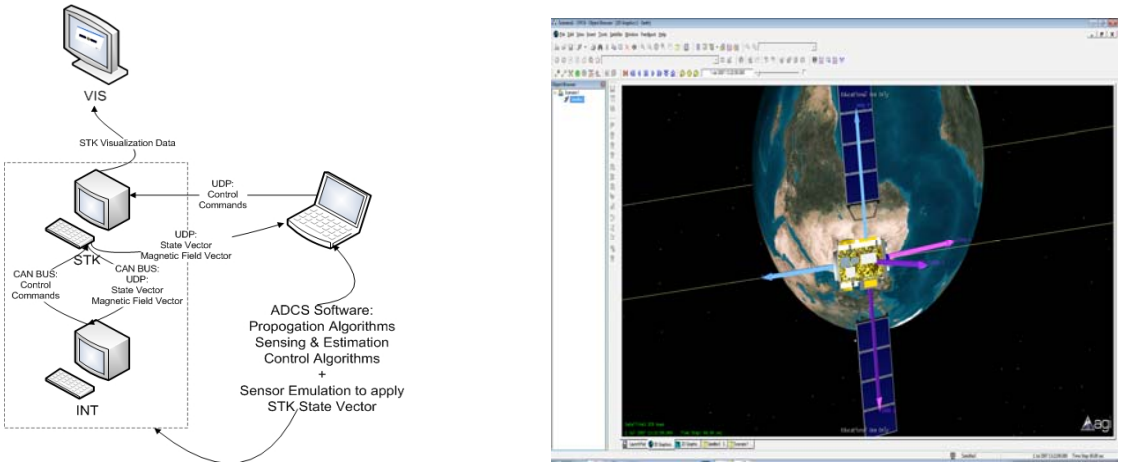

Fig. 14: *SIL System and STK Visualization*

Our experience on SIL simulations with iterative design resulted on control estimation and health management algorithms which are suitable for a nano sized satellite with three-axis precise attitude control.

B. HARDWARE-IN-THE-LOOP SYSTEM ARCHITECTURE

As the last step, actual hardware (sensor package, actuators and mission computer) is planned to be integrated into simulation environment along with experimental platforms. The main aim here is to test the integrated performance of the system under a realistic space environment (i.e. magnetic field and three axis micro-g motion). Towards this goal we have designed a HIL system. The computer rack system of the HIL consists of two rack PCs and one optional monitor which displays satellite simulation visual. The rack PCs not only simulate the S/C, environment, orbit and attitude propagation but also provide emulations of bus and sensor, retrieved by interface rack running MATLAB Simulink model. Interface Rack generates data updated by satellite hardware simulation system and STK Rack generates position and magnetic field values as in SIL (using another MATLAB Simulink model) as response and also displays satellites movements.

For simulating space environment, two primary components were integrated into simulation. First one is an in-lab-built frictionless air-bearing table to simulate spacecrafts attitude dynamics. The seconds one is a Helmholtz Coil system for simulating Earth's magnetic field on the orbit of the spacecraft. These coils are able to provide a homogenous magnetic field around spacecraft. When combined with air- bearing table, spacecraft should be able stabilize itself on the air bearing table via exerting torque with reaction wheels and magnetotorquers. The complete setup is illustrated in Fig. 15.

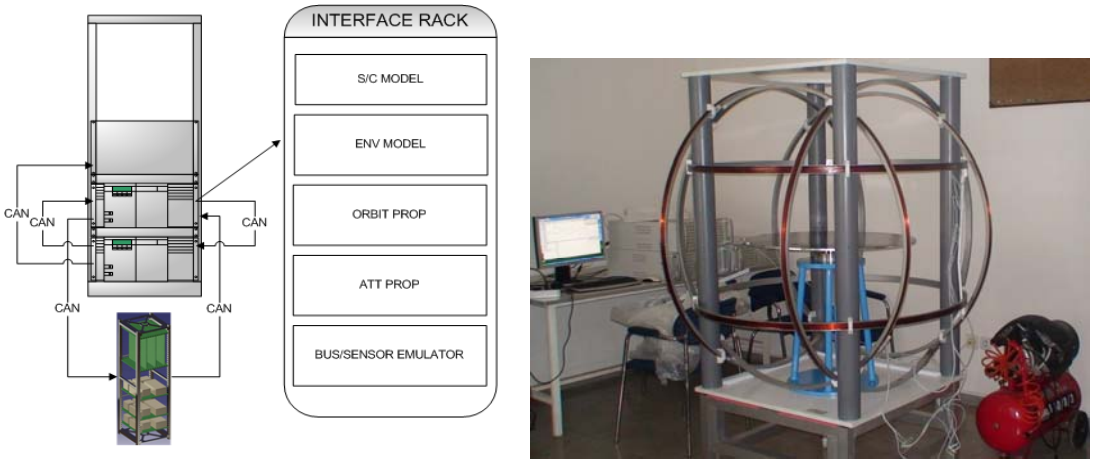

Fig. 15: *HIL system diagram and hardware : integrated air bearing table and helmholtz coil platform*

4. CONCLUSION

ITU pSAT II is the second student satellite project from ITU FAA Controls and Avionics Laboratory, which aims to design and on-orbit demonstrate a standardized bus and a novel ADCS for pico and nano sized satellites (1-10 kg) with multi objective applications. Main aim of this project is to demonstrate specific challenges and solutions for ADCS design for nanosatellites, which require a high precision, fault tolerant and reconfigurable control system. One of the bigger challenges in nanosatellite technologies is development of robust attitude determination and control systems which will allow these satellites' attitudes to be precisely known and controlled to obtain high quality mission data on demand. ITU pSAT II ADCS is envisioned to fulfill that requirement. ITU pSAT II is scheduled for launch on 2012 Q3.

In this paper, we presented the development stages of ITU pSAT II, focusing on the ADCS hardware and software implementations suited for high precision attitude control for small satellite. In addition, we presented the development of a SIL/HIL testbed which emulates the spacecraft dynamics and space environment.

This work is supported under TUBITAK 108M523 Project.

5. REFERENCES

[1] Can Kurtuluş, Taşkın Baltacı, Barış Toktamış, İlke Akbulut, O. Oğuz Haktanır, Gökhan İnalhan, , M.Fevzi Ünal ve A Rüstem Aslan, "İTÜ pSAT I: Getting Ready For Launch," Proc. of International Workshop on Small Satellites, Istanbul, Turkey, 2008.

[2] Can Kurtuluş ve Gökhan İnalhan, "Analysis of İTÜ NXG I Next Generation Technology Demonstrator from a Controls Perspective", Proc. Of 7th International ESA Conference on Guidance, Navigation & Control Systems, Tralee, Ireland, 2008.

[3] Can Kurtuluş, Taşkın Baltacı ve Gökhan İnalhan, "A Next Generation Test-Bed for Large Aperture Imaging Applications", Proc. of 21st Annual Conference on Small Satellites, Logan, ABD, 2007.

[4] Can Kurtuluş, S.M. İmre, G. Yüksel ve Gökhan İnalhan, "Technology Drivers and Challenges For Next Generation Distributed Spacecraft Systems", 3rd International Conference on Recent Advances in Space Technologies, İstanbul, Türkiye, 2007.

[5] Can Kurtuluş, Taşkın Baltacı, M. Ulusoy, B. T. Aydın, B. Tutkun, Gökhan İnalhan, N.L.O. Çetiner-Yıldırım, Turgut Berat Karyot, Cuma Yarım,F.O. Edis, C. Haciyev, A.R. Aslan ve M.F. Ünal, "İTÜ-pSAT I: Istanbul Technical University Student Pico-Satellite Program", 3rd International Conference on Recent Advances in Space Technologies, Istanbul, Turkey, 2007.

[6] http://polysat.calpoly.edu/

[7] http://courses.ece.uiuc.edu/cubesat/mission.htm

[8] http://www.und.nodak.edu/org/zamboni/

[9] http://www.conolley.com/cubesat/

[10] http://www.mae.cornell.edu/cubesat/

[11] http://space.auburn.edu

[12] http://www.css.tayloru.edu/~physics/picosat/indexes/purpose.htm

[13] http://www.space.t.u-tokyo.ac.jp/cubesat/index-e.html

[14] http://www.ssel.montana.edu/merope/mission/goals.html

[15] Jaime Esper, Peter V. Panetta , Dr. Michael Ryschkewitsch , Dr. Warren Wiscombe and Steven Neeck, 2nd IAA International Symposium on Small Satellites for Earth Observation NASA-GSFC nanosatellite technology for Earth science missions Acta Astronautica Volume 46, Issues 2-6 , January-March 2000, pp. 287-296

[16] Space Technology Guide, FY 2000-01, Department of Defense

[17] Hendrik Lübberstedta, David Koebela, Flemming Hansenb and Peter Brauerc, 4th IAA International Symposium on Small Satellites for Earth Observation MAGNAS-Magnetic Nanoprobe SWARM, Acta Astronautica Volume 56, Issues 1-2 , January 2005, pp. 209-212

[18] Robert Schulte, TUBSAT-N, an ultra low cost global communication nanosatellite system, Air & Space Europe, Volume 2, Issue 5, September-October 2000, pp. 80-83

[19] N.R. Gans, W.E Dixon, R. Lind and A. Kurdila, "Hardware in the loop simulation platform for vision based control of unmanned air vehicles", Mechatronics, 19, pp.1043-1056. 2009

[20] S. Rainer, K. Brieß and M. D'Ericco " Small satellites for global coverage: Potential and limits", ISPRS Journal of Photogrammetry and Remote Sensing, 2010

[21] Shiokawa, K. et al." ERG – A small-satellite mission to investigate the dynamics of the inner magnetosphere". Advances in Space Research, 38, pp. 1861-1869, 2006.

[22] Analytical Graphics STK/Integration. http://www.stk.com/products/by-producttype/applications/stk/add-on-modules/stk-integration

[23] H. Helvajian The generation after next: satellites as an assembly of mass-producible functionalized modules. In H. Helvajian & S. Jason (Eds.), Small satellites: past, present, and future . Aerospace Press. 2009

[24] Laurent Marchand, John Hopkins, Fabien Filhol, Micro and Nano Industry Space Days, ESA/ESTEC, 30 May 2006

[25] Neil Barbour and George Schmidt, Inertial Sensor Technology Trends, IEEE Sensors Journal, Vol. 1, No. 4, December 2001

[26] Peter Rossoni, Peter V. Panetta, Developments in Nano-Satellite Structural Subsystem Design at NASAGSFC, 13 th AIAA/USU Conference on Small Satellites

[27] V.J. Lappas , WH Steyn , C.I. Underwood, Attitude control for small satellites using control moment gyros, Acta Astronautica, Volume 51, Issues 1-9, July-November 2002, pp. 101-111

[28] Demoz Gebre-Egziabher, Gabriel H. Elkaim, J. D. Powell and Bradford W. Parkinson, A Gyro-Free Quaternion-Based Attitude Determination System Suitable for Implementation Using Low Cost Sensors, Position Location and Navigation Symposium, IEEE 2000

[29] M.L. Prydderch, N.J. Waltham , R. Turchetta , M.J. French , R. Holt , A. Marshall, D. Burt , R. Bell , P. Pool , C. Eyles , H. Mapson-Menard, A 512512 CMOS Monolithic Active Pixel Sensor with integrated ADCs for space science, Nuclear Instruments and Methods in Physics Research A 512 (2003) pp. 358-367

[30] N. K. Ure, Y. B. Kaya, G. Inalhan, The Development of a Software and Hardware-in-the-Loop Test System for a Reconfigurable and Fault-Tolerant Nano-Satellite Attitude Determination and Control System: ITU-PSAT II ADCS, 2011 IEEE Aerospace Conference, March 5–12 2011, Big Sky, Montana, 2011

[31] U. Eren, Attitude Determination and Control System Design for Nanosatellites, B.Sc. Thesis, Istanbul Technical University, Faculty of Aeronautics and Astronautics, 2011

[32] E. Koyuncu et. al., ITU-pSAT II : 5th High precision Nanosatellite ADCS Development Project, International Conference on Recent Advances in Space Technologies, 2011,Istanbul,Turkey

[33] The Cubesat Program, Cal Poly SLO, Cubesat Design Specifications Rev.12, 2011